An experimental analysis of self-*Q*-switching via stimulated Brillouin scattering in an ytterbium doped fiber laser

2013 Laser Phys. Lett. 10 055112

(http://iopscience.iop.org/1612-202X/10/5/055112)

Laser Phys. Lett. **10** (2013) 055112 (10pp) doi:10.1088/1612-2011/10/5/055112

LETTER

An experimental analysis of self-*Q*-switching via stimulated Brillouin scattering in an ytterbium doped fiber laser

Alexander V Kir'yanov[1,2,4], Yuri O Barmenkov[1] and Miguel V Andres[3]

[1] Centro de Investigaciones en Optica, Loma del Bosque 115, Col. Lomas del Campestre, 37150, Leon, Guanajuato, Mexico
[2] A M Prokhorov General Physics Institute of the Russian Academy of Sciences, Vavilov Street 38, 119991, Moscow, Russian Federation
[3] Departamento de Física Aplicada—ICMUV, Universidad de Valencia, Dr. Moliner 50, 46100, Burjassot (Valencia), Spain

E-mail: kiryanov@cio.mx

Received 18 September 2012
Accepted for publication 11 February 2013
Published 16 April 2013
Online at stacks.iop.org/LPL/10/055112

Abstract
An experimental study of self-*Q*-switching (SQS) in an ytterbium doped fiber laser (YDFL) arranged using a twin-core GTWave assembly is reported. The main mechanisms that initiate, amplify, and limit SQS pulses in amplitude are revealed to be stimulated Brillouin and Raman scattering (SBS/SRS) and Yb^{3+} amplified spontaneous emission. The parameters featuring SQS oscillation in terms of efficiency and stability of pulsing are found to be intra-cavity loss and feedback strength. An analysis of the YDFL SQS regime's features—pulsing time series, optical and RF spectra, amplitude and timing jitter—is provided for the two experimental situations: (i) when SQS pulsing stochastically intermits with regular active *Q*-switching pulses, given by the action of an intra-cavity acousto-optical modulator, and (ii) when a pure SQS mode is intentionally implemented in the YDFL without a modulator. The close relationship of the processes involved and SQS parameters in these two circumstances is demonstrated. Giant pulses with durations of 70–80 ns are shown to be generated at threshold intra-cavity powers of around 250 W (SBS threshold) and limited at approximately 2 kW of peak power (SRS threshold). At SBS-SQS, we show that at high values of intra-cavity loss, and thus reduced feedback, the amplitude and timing jitter values can be reduced to 5% and 7%, respectively.

(Some figures may appear in colour only in the online journal)

1. Introduction

Q-switched ytterbium doped fiber lasers (QS-YDFLs) producing powerful pulses in the nanosecond range are attractive light sources for applications in many areas, such as laser marking and cutting [1], super-continuum generation [2–4], nonlinear frequency conversion [5, 6], etc. The significant features of such lasers are a long interaction length of the pump light with an active fiber, which permits reaching a high fiber gain, high laser efficiency, and single transversal mode operation, all important in practice. Another

[4] On leave from A M Prokhorov General Physics Institute of the Russian Academy of Sciences.

–negative—feature of QS-YDFLs is pulse jitter, observed mostly in passively QS lasers [7, 8], which degrades the regime quality.

Much research has been reported concerning measures to reduce pulse jitter in lasers, among which are the use of a composite pump scheme [9], optical triggering of saturable absorbers [8, 10], hybridization of active and passive QS [7], and external injection [11].

One of the important causes of pulse jitter in QS-YDFLs is stimulated Brillouin scattering (SBS), a stochastic process in nature. Since SBS is characterized by a comparatively low threshold, from several tens to a few hundreds of watts in conventional (not large-mode-area) fibers, it frequently accompanies operation of an YDFL in active and passive QS modes when the pulse power exceeds the SBS threshold [12–16]. Recently it has been shown that SBS-induced pulses may occur in YDFLs with a low Q-factor of laser cavity in which neither a saturable absorber nor any active QS cell is placed [15, 17].

The present letter reports an experimental analysis of the two versions of an YDFL with double-clad pumping, both implemented in a standard Fabry–Perot configuration, where (i) SBS-induced SQS pulsing interferes with regular pulses produced by an intra-cavity acousto-optical modulator (AOM) (the first version) and (ii) pure SQS pulsing, realized through the inherent SBS process in the absence of AOM (the second version). For the first YDFL, we reveal the detrimental role of SBS-SQS pulsing when targeting AOM-induced QS. The second YDFL was analyzed mainly in terms of both amplitude and timing jitter, inevitable at SBS, and the measures applied to reduce them; in particular, a detailed statistical analysis of deviations in pulse amplitude and inter-pulse interval; this allowed us to reveal that the instabilities in SBS-SQS pulsing are mainly related to the cavity loss factor.

In the experiments, GTWave ('twin-core') Yb^{3+} doped fiber (GTW-YDF) fiber, an attractive kind of double-clad pumping arrangement [18], was used. To date, such fibers have been extensively explored, covering a wide range of possible applications (see e.g. [19–26]), but as far as we know no comprehensive studies regarding the SBS-SQS regime's features in an YDFL based on a GTW-YDF assembly have been made.

2. AQS and SBS-SQS mechanisms of pulsing in YDFL with AOM in the cavity

We first explored a diode-pumped actively *Q*-switched (AQS) YDFL implemented in a standard arrangement. Insight into its operation allowed us to reveal certain remarkable unexpected features. In particular, we found that, at low modulation frequencies of an intra-cavity acousto-optic modulator (AOM), peculiar SBS-induced SQS (further—'SBS-SQS') pulsing is present in the laser, which intermits with regular AQS pulses. Furthermore, at increasing modulation frequency, SBS-SQS pulsing was seen to gradually vanish while regular AQS pulsing remained. Pulses that were lased as a result of the SBS-SQS process are much more intense and short as compared to those resulting from AQS. Importantly,

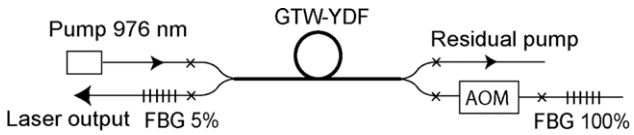

Figure 1. Experimental setup: the YDFL oscillating with mixed AQS/SBS-SQS. The YDF length is 6.5 m; total length of all other intra-cavity elements is 2.5 m. Crosses indicate fiber splices.

the first type of pulses, initiated in the cavity through the stochastic SBS process from noisy ASE and amplified by weak reflections from the AOM, arise in the time intervals when the AOM is in the OFF state, whereas the second type (true AQS) of pulses developed when AOM is in the ON state. Thereafter, the presence of the two types of pulsing in the YDFL (at low AOM modulation frequencies) resulted in significant instabilities of the laser output.

The YDFL was implemented in an all-fiber configuration, sketched in figure 1.

We used as an active medium the GTW-YDF, which consists of two in-stack coupled fibers, one of them being multimode undoped pump fiber with a core diameter of 110 μm and the other being Yb^{3+} doped (active) fiber with a core diameter of 11 μm, cutoff wavelength of 1.05 μm, and Yb^{3+} concentration of 8.5×10^{19} cm^{-3}. The outer diameters of both fibers forming the GTWave assembly are 125 μm. The effective absorption of pump light evanescently coupled from the pump to the active fiber was measured to be 1.6 dB m^{-1} at 976 nm; back-coupling of the signal radiation from the active to the pump fiber is negligible in the GTWave design. A fiber-coupled 976 nm semiconductor laser with a maximum power of 4.0 W was used to pump the GTW-YDF through a splice (multimode fiber of the pump laser had the same diameter, 110 μm). The length of the GTW-YDF was chosen to be 6.5 m, which provides effective pump-light absorption over the entire active fiber length. The YDFL cavity was formed by two fiber Bragg gratings (FBGs) with reflection coefficients of 5% (output) and 100% (rear), both centered at 1080 nm and both having bandwidths around 100 pm. The total laser cavity length was about 9.5 m. AQS was built up due to ON–OFF action of the AOM (the Gooch & Housego version) placed between the Yb^{3+} doped fiber and 100% FBG. The key characteristics of the AOM are as follows: operation wavelength—1030–1090 nm; driving acoustical frequency—111 MHz; insertion loss—4 dB/pass; back reflection——35 dB. The YDFL's output (5% FBG) was monitored using either an optical spectrum analyzer (OSA) or a high-frequency photodetector (1.2 GHz bandwidth), connected to a fast digital oscilloscope (2.5 GHz bandwidth) or to a RF spectrum analyzer (0–100 kHz bandwidth).

The SBS-SQS regime, characterized by powerful, short pulses, or 'bursts', occurs in this arrangement at repetition rates $f_m < 39$ kHz at the time instants when the AOM is in OFF state; see figures 2(a)–(d). Interestingly, at f_m below 27 kHz (figures 2(a)–(c)), SBS-induced SQS is a sole pulsed regime observable in the YDFL whereas at f_m tuned within an interval 27…38 kHz the SBS-SQS regime is intermitted with the common AQS one, characterized

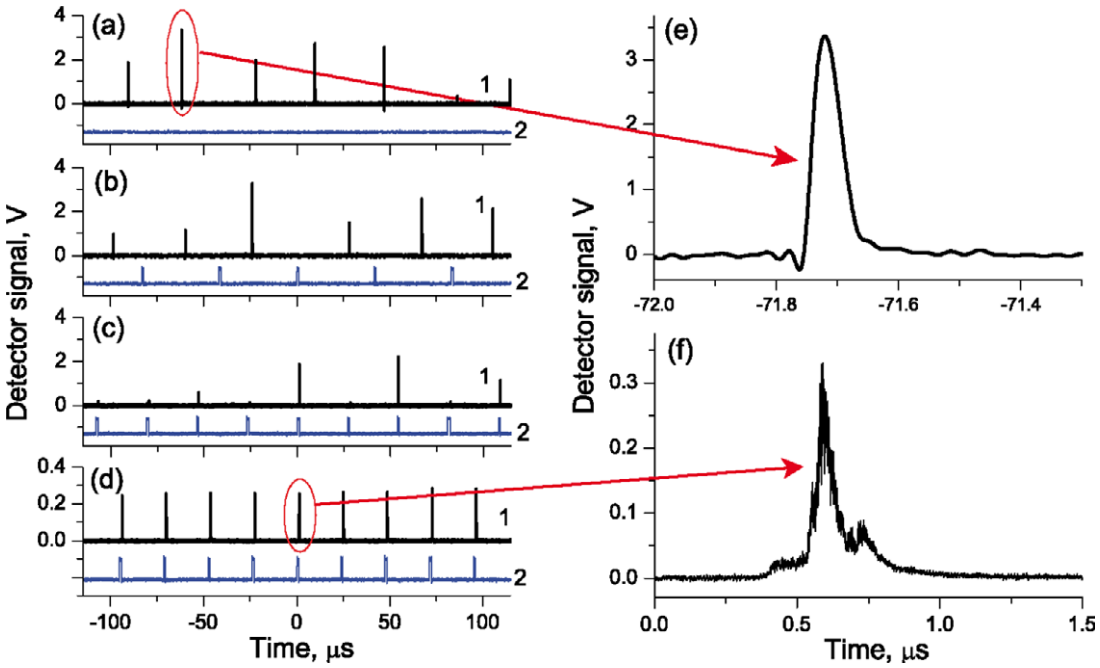

Figure 2. Laser output after 5% FBG (black curves 1) at different AOM modulation frequencies: (a) 0, (b) 24, (c) 37, and (d) 40 kHz (blue curves 2 are the control signals applied to the AOM driver). Note that the output scale at the lowest snapshot (d) is zoomed, relative to the rest of the snapshots (a)–(c), to guide the eye on AQS pulses. Insets show typical images of pulses in SBS-SQS (e) and AQS (f) sub-regimes. In the experiments, the AOM's gate (transparency window) was always set to 2 μs.

by less intense and longer pulses; that is, SBS-SQS and AQS operations at these modulation frequencies coexist but compete to consume inversion accumulated in Yb^{3+} system. Notice that similar, SBS- or more complicated SBS/stimulated Rayleigh-scattering related, regimes are known to occur in YFDLs with a low Q-factor of the cavity. In our case, overall round-trip losses at AOM being in OFF state are around 48 dB, which are produced by loss inside the AOM unit and by small reflections from the 5% FBG. Apparently, such high intra-cavity loss values allow the establishment of a high inversion level in the active Yb^{3+} fiber, which is released through a stochastic SBS process in the form of powerful (peak power of around 2 kW), short (around 70–80 ns at a 3 dB level) pulses. The other essence of the SBS-SQS regime is the chaotic distributions of both the pulse amplitude and intra-pulse spacing in the time domain; we inspect these in more detail in section 3. Worth noticing is the temporal shape of such pulses (figure 2(e)), inherent to the SBS mechanism involved. However, of a quite different kind are the parameters of common AQS pulses that are intermitted with the SBS ones. In figures 2(c) and (d), these are lower amplitude 'regular' pulses that appear within the intervals when the AOM is in the ON state. The regular AQS pulses have peak powers of less than 180 W and durations of about 0.3 μs. Their temporal shape is also quite characteristic (see figure 2(f)) and similar to the pulse shape usually obtained at AQS. It is worth mentioning that, at an increasing AOM repetition rate within an interval $f_m = 27 \ldots 38$ kHz, SBS-SQS pulses become less and less probabilistic, whereas regular AQS pulses appear to be more and more pronounced and stable (compare figures 2(a)–(d)).

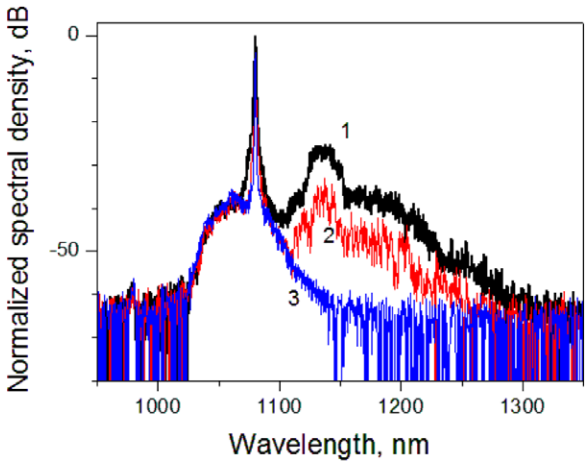

Figure 3. Optical spectra measured from the YDFL at different AOM modulation frequencies (OSA resolution is 1 nm). Curve 1 corresponds to zero AOM modulation frequency (AOM is blocked), curves 2 and 3 correspond to modulation frequencies of 35 and 40 kHz, respectively.

The other noticeable thing is the peculiar character of the transformations in the optical spectra of the YDFL, which were detected with increasing AOM modulation frequency; see figure 3.

It is seen that, in a broad range of f_m (from DC—when the AOM is always blocked—up to 30 kHz), the optical spectra change insignificantly: compare black curve 1 and red curve 2 in figure 3. In these spectra, a sharp laser peak (at the central wavelength of FBGs) and several smoother Stokes peaks that correspond to the stimulated Raman scattering

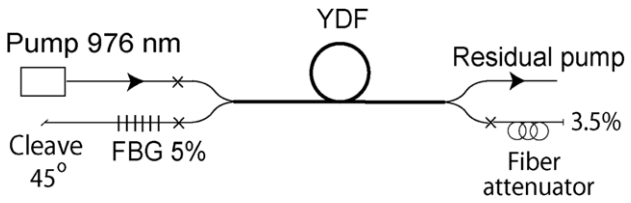

Figure 4. Experimental setup (YDFL at pure SBS-SQS). The YDF length is 6.5 m, crosses mark fiber splices.

(SRS) process, obtained by inversion in the Yb^{3+} system, coexist. But at increasing f_m from about 30 kHz, these Stokes peaks gradually decrease in magnitude until they disappear completely at $f_m \geq 39$ kHz. This fact, after comparing with figure 2, becomes understandable: indeed, within this f_m interval the YDFL shifts from the mixed SBS-SQS to pure AQS, with the pulse amplitude in the latter regime being much less than in the former. Such noticeable transformations in the YDFL optical spectra, rather swift (compare curves from 1 to 3 in figure 3), arise when the AQS pulse peak power becomes too small (<180 W) to reach the SBS threshold (around 250 W) for our GTW-YDF having a core diameter of 11 μm. Furthermore, from spectrum 3 in figure 3 (which corresponds to regular AQS pulses, refer to figure 2(d)), we can estimate the ASE contribution to the YDFL output. It was found to be negligibly small (<2%) as compared with the total output power averaged over many pulse cycles. Also apparent is the peak power level at which the amplitudes of SBS-SQS pulses are limited (nearly 2 kW; see above): this is the characteristic power at which the SRS process becomes effectively developed in the core area of the YDF.

Concluding this part, we emphasize that if the AOM is always blocked (figure 1) the laser nonetheless sporadically oscillates with SBS-SQS pulses (see figure 2(a)); this means that in this case a laser cavity is formed by the 5% FBG and the internal, extremely small, back reflections from the blocked AOM, provided a high inversion in the active Yb^{3+} doped fiber has been stored at high pumping. This forced us to explore the YDFL in the circumstance of a 'bad cavity' [17, 27] without an AOM inside, which is the topic of section 3.

3. SBS-SQS pulsing in YDFL without AOM

The physics behind 'pure' SBS-SQS pulsing can be clarified from an analysis of the YDFL implemented in the configuration drawn in figure 4.

Notice that this YDFL version was built using almost the same elements that were featured above (section 2). The few changes we made are (see figure 4): (i) the AOM was removed from the YDFL cavity; (ii) a short piece of standard HI980 fiber forming a hand-made tunable attenuator (TA) was spliced to the active YDF instead of the 100% FBG, the free end of which was cleaved, giving a normal (90°) cut with ~3.5% broadband coupling; (iii) the free end of the other coupler (fiber with 5% FBG inside) was cleaved at ≈45° to minimize non-resonant reflection back to the cavity. The reasons for handling such an YDFL configuration were, first, to inspect the details featured at pure SBS-SQS pulsing, not affected by the AQS (AOM) action (e.g. the immanent pulse instabilities against the key laser parameters) and, second, to characterize the SBS-SQS regime in terms of variable intra-cavity loss and pump power. Apparently, this knowledge should be valuable for any kind of double-clad pumped YDFL.

If the overall intra-cavity loss is comparatively high (>15 dB) but does not exceed a certain value, about 65–67 dB, the YDFL in the latter configuration operates in a pulsed regime resembling the one described for the YDFL in section 2, where little or no effect was produced by the AOM: refer to figures 2(a)–(b) and 3 (spectra 1 and 2).

Figures 5–7 exemplify such a regime at 46 dB intra-cavity loss, a value comparable with the total loss in the previous YDFL arrangement when the AOM was in the OFF state.

In figure 5 we show snapshots of SBS-induced pulsing and the corresponding RF spectra measured at the YDFL output (5% FBG) at various pump values. It is seen that regularity of SQS pulsing is enhanced with increasing pump level, compare snapshots (a) and (b) in figure 5, while the pulse repetition rate grows, see RF spectra (c)–(f) in this figure. One sees from the spectra that the RF peaks become narrower with increasing pump power, an indication of enhancement of the SQS regime's quality in terms of amplitude and repetition rate stability.

Optical spectra of the YDFL laser in the version of figure 4 are shown in figure 6.

The threshold of SBS-SQS lasing in this configuration is around 1.1 W; below this value an Yb^{3+} super-fluorescent regime is observed in the system, sampled by curve 1 in figure 6, whereas just above threshold pulsed lasing is suddenly established. It is seen that the shape of the optical spectra remains virtually constant with increasing pump level; compare curves 2–5 in figure 6. The central wavelength of lasing is always at 1080 nm, the wavelength established by the 5% FBG coupler, which therefore reveals a non-vanishing role of the coupler and so of feedback in 'igniting' the laser action. The Raman process (of the first and second orders—see spectral peaks located at nearby 1140 and 1180 nm) is clearly seen to contribute to lasing at any pump power: compare the spectra in figure 6 with the ones shown in figure 3. Thus, Raman scattering is apparently a mechanism that limits the pulse amplitude at an approximately 2 kW level, the characteristic power for SRS in the present experimental conditions, likely in the previous laser version (see section 2).

An important aspect of the SBS-SQS regime is pulsing instability. Figure 7 allows one to capture its main features.

At the chosen parameters of the YDFL (46 dB overall loss and 4 W pump power), neither of the irregularities—in the peak power (a) and timing jitter (interval between the adjacent pulses) (b)—are significant. Figure 7(c) shows the interrelation between these two kinds of instability. It is seen that there is a tightly segregated confidence area of quite small jitter (±5% for amplitude and ±10% for timing jitters) where the SBS-SQS regime can be regarded to be relevant for applications. Figure 7(d) shows a typical pulse taken from the train shown in figure 5(b); notice that pulse width is a rather stable value, being confined within a 70–80 ns interval.

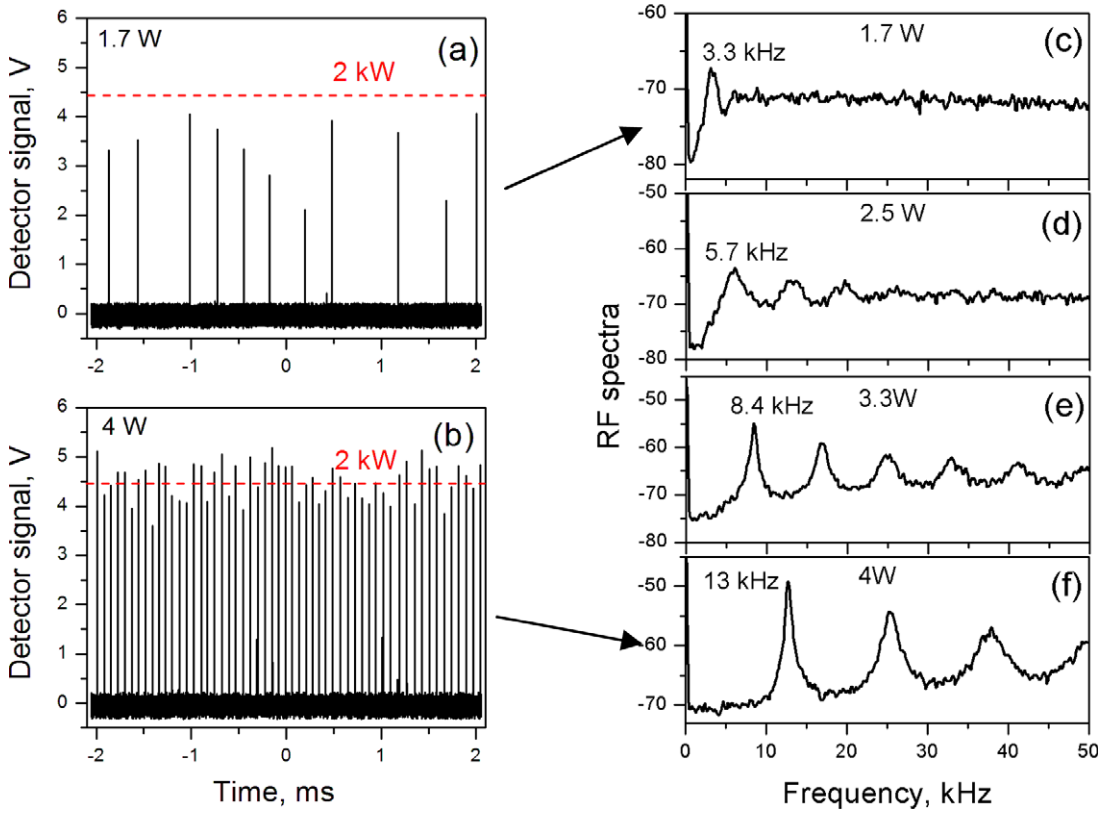

Figure 5. Left (a), (b) plots are typical SBS-SQS snapshots (oscilloscope traces) obtained at the YDFL output (5% FBG) at two pump powers: (a) 1.7 W and (b) 4.0 W. The red dashed lines show the level corresponding to 2 kW of peak power. Right (c)–(f) plots are RF spectra of lasing, measured at four pump powers: (c) 1.7 W, (d) 2.5 W, (e) 3.3 W, and (f) 4.0 W. The correspondent pulse repetition rates are indicated near the first RF peaks (the fundamental harmonics of the pulse RF spectra). All the data are acquired at an overall intra-cavity loss of 46 dB.

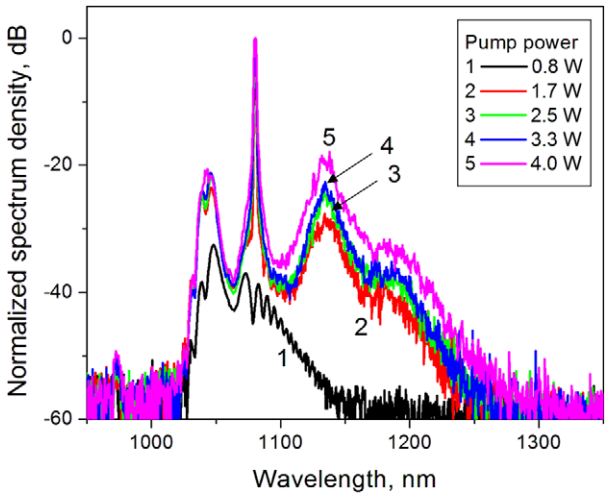

Figure 6. Optical spectra measured from the YDFL at different pump powers and 46 dB loss level (OSA resolution is 1 nm). All the spectra are normalized to the maximum obtained at 4 W pumping.

This shows clearly that, similarly to the results reported in section 2, the threshold of SQS pulsing is around 250 W (the typical value at which the SBS process starts up) whilst pulse amplitudes are limited by approximately 2 kW (the typical value at which the SRS process is developing), thereafter revealing the most relevant physical sides of SBS-SQS oscillation.

The other illustration of the YDFL demonstrating pure SBS-SQS is given by figure 8.

It is seen that a much more unstable pulsed regime occurs in the case when TA is tuned to a significantly reduced loss value (27 dB). At the same (maximal) pump power, 4 W, giant pulses drastically fluctuate in amplitude and suffer from a pronounced timing jitter, figure 8(a). It is also seen, figure 8(b), that the optical spectra of lasing resemble the reported ones for 46 dB loss; however, once compared with figure 6, they are seen to have a more notable dependence on a pump level. But, as can be easily understood, the differences are simply the appearance, within intermitting time intervals between SBS-related pulses at low pump powers, of longer and longer ones, resembling a transient behavior at CW pumping; refer again to figure 8(a). Further, the diagrams of amplitude and timing jitter, see figures 8(c)–(d), are more complicated than those in the previous case; compare with figures 7(a)–(b). The two maxima in the histogram on figure 8(c) originate from the presence in the train of a section of pulses that is not affected at all by the SRS process (the left maximum), whilst another section of pulses suffer to varying degrees from it (the right maximum). Also notice a different kind of histogram for time intervals between the pulses (figure 8(d)), namely, concentrating of pulses in the

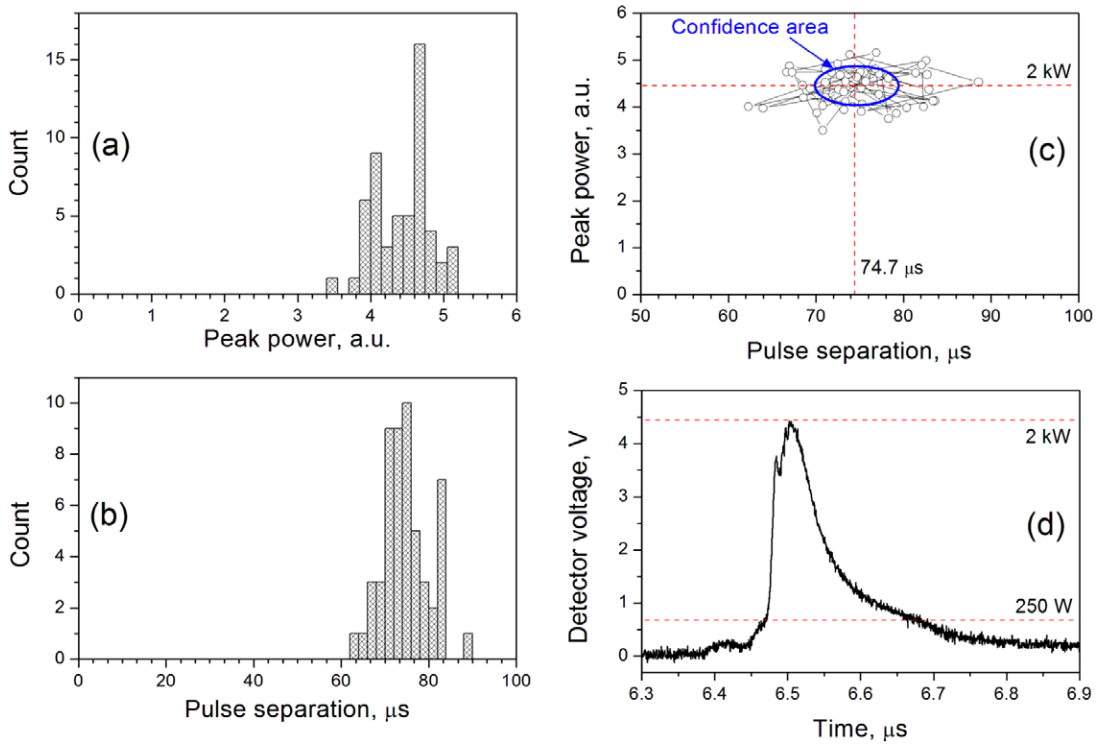

Figure 7. (a), (b) Histograms of pulse number distributions in the domains of peak power (amplitude jitter, (a)) and pulse separation in time (timing jitter, (b)). (c) The cross-relation between jitters, featuring the confidence area for the parameters. (d) A typical SBS-SQS pulse portrait. All the data are acquired at a 46 dB intra-cavity loss and 4 W pump power.

train near a separation time value much lower (a few to 30 μs) than in the previous case (60–80 μs; figure 7(b)). Most probably, a physical explanation for such a trend to exist is that the much lower intra-cavity loss in the current case (27 dB instead of 46 dB; see figures 5–7) does not permit accumulation of inversion in the Yb^{3+} system, making it incapable of reaching the Raman threshold (2 kW) or even the SBS threshold. An illustration of the latter is the diagram shown in figure 8(e), which shows the interrelation between the amplitude and timing jitters, where one cannot distinguish any definitive confidence area for pulses, unlike in the preceding example (compare with figure 7(c) for a 46 dB loss factor).

Let us analyze the results obtained with the SBS-SQS YDFL version without the AOM, collected for a variety of intra-cavity loss levels; figure 9.

From figure 9(a) it is seen that, at 4 W pumping (the maximal pump level in our experimental conditions), pulse width and repetition rate are both functions of intra-cavity loss. Namely, for higher loss factors (we changed it by manipulating the TA), shorter pulses and lower repetition rates are obtained. The captured law holds for a wide range of intra-cavity loss factors (10...50 dB), thus featuring a general trend given by interplay of the internal SBS/SRS processes involved. Meanwhile, as stems from the results reported above, the most attractive is the SBS-SQS scenarios occurring at a comparatively high loss level (35...55 dB), when the stability of the output pulses is maximum. Schematically, this range is on the right side of the separating blue line in figure 9(a).

Further, as seen from figure 9(b), the amplitude stability of SBS-SQS pulses increases drastically with increasing cavity loss: the normalized standard deviation (NSD) drops from 16% to 5% when the cavity loss factor is increased from 27 to 46 dB. An interesting fact is that the experimental points are fitted well by the linear regression when presented in a double-logarithmic scale; giving the law for the dependence in figure 9(b) as follows: NSD $\sim \exp[-(0.1 \times \text{loss[dB]})]$. Another interesting point is an estimate found after extrapolation of the dependence of NSD on loss to higher values of the latter. It is seen that one would expect a further drop in NSD to ~2.3% at ~65 dB, the limiting value at which SBS-SQS pulsing is still observed (see below).

Interesting insights into the physics involved can be made after analyzing the optical spectra; see figure 9(c). In this figure, we show how these spectra look at some characteristic levels of intra-cavity loss (the spectra were registered at the 5% FBG output). It is seen that (i) if intra-cavity loss is extremely high then no lasing exists at all and inversion accumulated in the active fiber is released in the form of ASE (curve 5); (ii) if the loss is extremely small then no regular pulsing exists but instead a quasi-CW oscillation with low amplitude and irregular spiking is observed, with a narrow line centered at 1080 nm (given by the presence of the 5% FBG) on an ASE pedestal (curve 1); (iii) if the loss is tuned to be within the range where stable SBS-SQS pulses are observed, the optical spectra of lasing (curves 2–4) become similar to the ones reported above (compare with figures 6 and 8(b)).

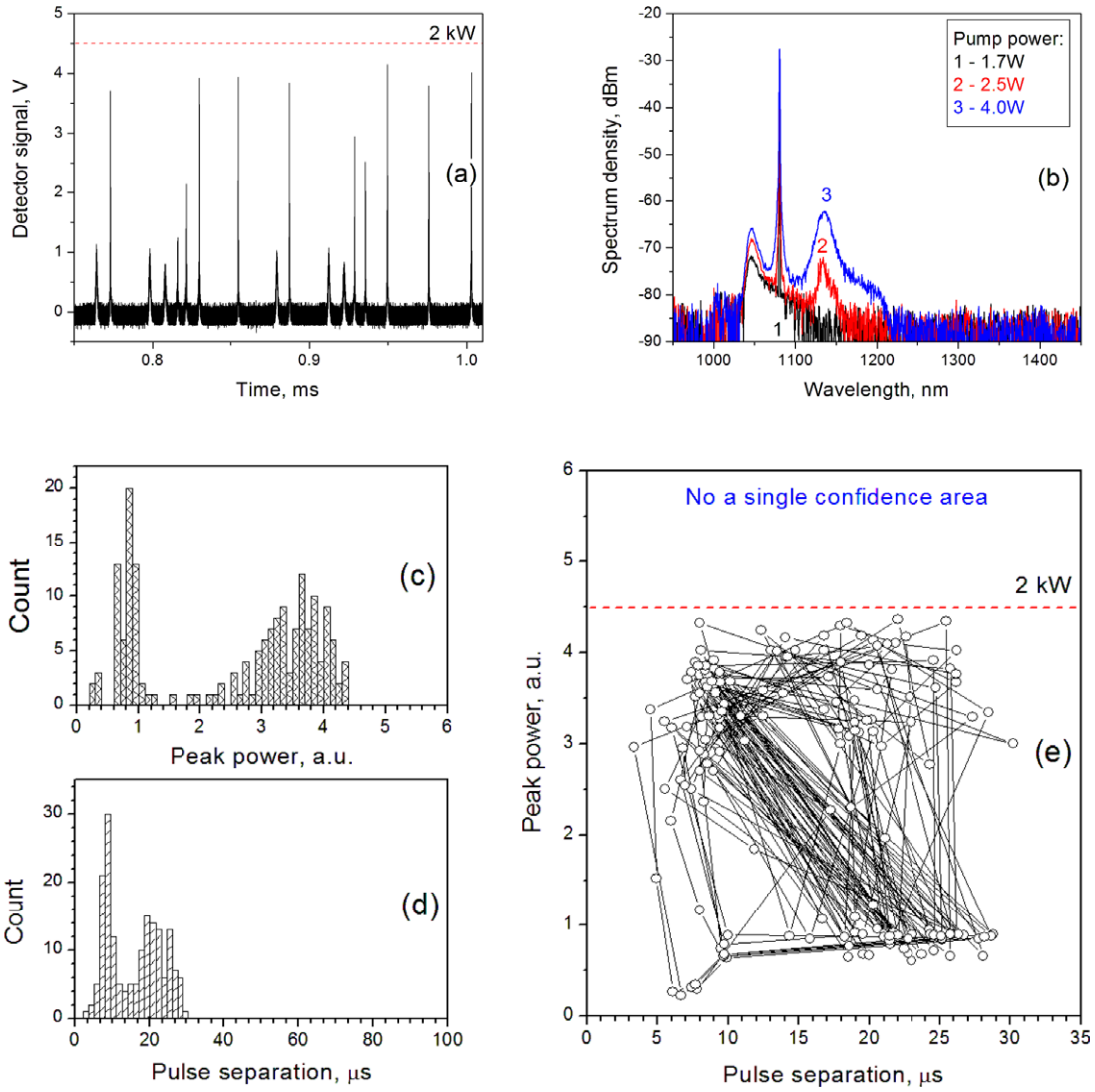

Figure 8. Characterization of the YDFL output (after 5% FBG) at 4 W pump power and 27 dB overall intra-cavity loss. (a) A snapshot of pulsing (oscilloscope); (b) optical spectra measured at different pump powers (OSA resolution is 1 nm); (c), (d) histograms of pulse counts in the domains of peak power (amplitude jitter, (c)) and pulse separation in time (timing jitter, (d)); (e) cross-relation of the jitters. Red dashed lines in figures (a) and (e) show the SRS limit (2 kW).

4. Discussion

The reported results certainly allow insight into significant aspects of spontaneous (SQS) pulsing, established in an YDFL as a result of the SBS process. Generally speaking, SBS-related spiking in YDFLs has been known for long time and much research has been directed so far towards its exploration and understanding; see the references mentioned in section 1 and also [28–31]. Moreover, the SBS process was extensively studied when producing SBS-based fiber lasers; see e.g. [32, 33].

As far as we know, the situation treated in section 2—when SBS-SQS arises as spontaneous pulsing in an intentionally AQS YDFL (namely, using an intra-cavity AOM; see figure 1)—is addressed here in detail for the first time. The inevitable and detrimental role of SBS-induced pulsing in the form of short and intensive bursts that interrupt sequences of regular AQS pulses was clearly shown to occur at the time intervals when the AOM is in the OFF state. This holds either at low AOM modulation frequencies, measured in a few to tens kHz, or even with the AOM always closed (see figure 2). The other important property found regarding this regime is that the amplitude of SBS-induced pulses is apparently limited by the SRS process, which is evidenced by the optical spectra of lasing (see figure 3).

The results reported further clarify the matter of SBS-SQS pulsing in a situation where no AOM is utilized in the YDFL (figure 4). Throughout, the roles of SBS (as a starting mechanism) and SRS (as a limiting one) were proved for 'pure' SBS-SQS pulsing (see figures 6 and 7(d), and 8(b)) and at the same time the instabilities inherent to the stochastic nature of SBS/SRS processes were explored (see figures 5, 7 and 8). However, most of our attention was paid to investigating the essence of SBS-SQS pulsing in terms of intra-cavity losses, the results summarized in figure 9. To the best of our knowledge, this matter has also remained

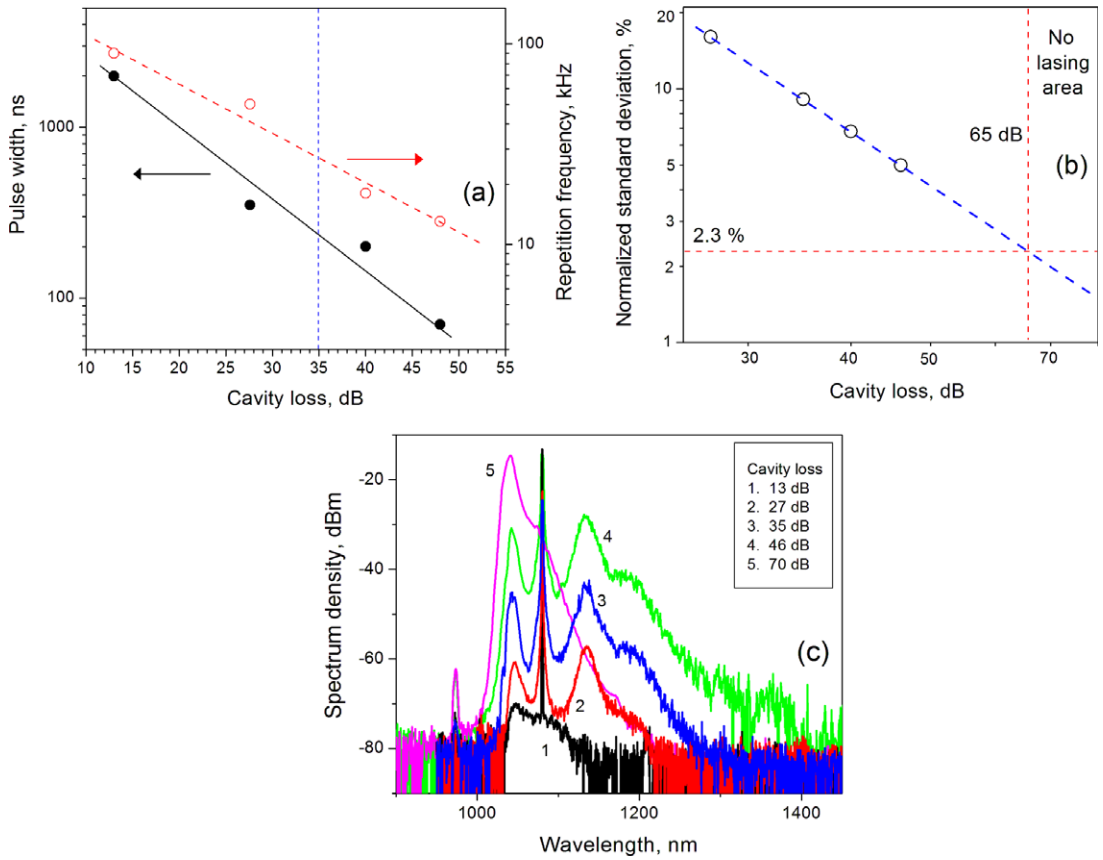

Figure 9. (a) Dependence of pulse width and repetition rate of SBS-SQS pulsing on intra-cavity loss. Circles show the experimental values and dashed black and red lines show their fittings. The blue line segregates the loss regions with stable (right) and irregular (left) pulsing. (b) The NSD of the amplitude of SBS-SQS pulses as a function of overall intra-cavity loss. (c) Typical optical spectra obtained from the laser at different (from 13 to 70 dB) loss levels; see the text for more details. All data were obtained at 4 W pump power.

untouched in the literature on SBS-SQS in YDFLs. It was found that a high loss level attained in the cavity (see the region in figure 9(a) to the right side from the vertical dashed line) ensures a high inversion is created in the Yb^{3+} system, which allows—if a non-vanishing feedback is present—the release of accumulated energy in the form of short, intense pulses via the SBS process, rather than in the form of CW (or quasi-CW) lasing. On the other hand, an intra-cavity loss factor should not be so high as to prevent release of the stored energy in the form of ASE. Otherwise, if a small loss level is the case (see the region in figure 9(a) to the left side from the vertical dashed line), the YDFL either emits extremely unstable pulses or operates in quasi-CW. All of these scenarios are clearly illustrated by the optical spectra shown in figure 9(c).

One more thing to mention is that, despite high loss in the YDFL cavity being revealed as a crucial requirement for stable SBS-SQS pulsing, the necessity of a feedback [34] (even a 'bad' one) is itself a requirement (otherwise no lasing is observed at all in the system). The latter is in turn a prerequisite of narrow-line lasing at SBS-SQS; see the optical spectra in figures 6 and 8(b), and 9(c). Thus, the SBS process seems to be capable of producing SQS as an effective boost of a preliminary (and properly) 'prepared' spectrally narrow burst, given by the high spectral selectivity of a FBG coupler.

Also worth noticing is that in our case the duration of pulses generated at SBS-SQS (70–80 ns) is always equal to the average of one round-trip of light in the cavity, indicating a regenerative amplifier behavior of the system under examination rather than a classical laser behavior.

Finally, we can hypothesize here that the true physical reason for effective SBS-SQS pulsing in our fiber system resembles that suggested long ago when studying SQS solid-state bulk lasers with an outer or inner SBS-active liquid cell; see [35]. The milestone result [35] was that SBS-SQS occurs in a laser when a transition occurs from an unstable resonator (with high loss, in absence of a SBS 'mirror') to a stable one (after creating by intra-cavity radiation of a phase-conjugating SBS 'mirror'). Needless to say, a quite similar physical situation should take place with our YDFL. That is, SBS-SQS pulsing is established at a transition from the low-Q cavity (while the SBS process was developing) to the high-Q cavity (after the SBS process has created additional feedback with a reflectivity as high as almost 100%). In other words, SBS plays the role of an intensity-dependent reflector inside the 'bad' (low-Q) cavity of the YDFL, thereafter acting as a Q-switching mechanism. Such an illustration of what happens physically with the YDFL under examination helps in gaining a clearer understanding of the nature of the SBS-SQS regime.

5. Conclusions

The present Letter focuses on a detailed study of the self-*Q*-switching (SQS) regime in an all-fiber laser based on a Yb-doped GTWave twin-core structure, GTW-YDFL. We inspect such parameters of the pulsed SQS regime as pulsing time series, optical and RF spectra, amplitude and timing jitter, with regard to the key factor determining it—the intra-cavity loss. The SBS process, well-known from previous studies as a factor triggering SQS in an Yb-doped fiber, together with the SRS process as a factor limiting peak power of output pulses, are experimentally explored and discussed.

Starting our analysis with an insight into the operation of the GTW-YDFL with an acousto-optical modulator (AOM) in the cavity at low repetition rates (DC—tens kHz), we showed that the laser changes to a regime where regular—via active *Q*-switching (AQS)—pulses, arising due to the AOM action, are intermitted with SQS pulses generated stochastically through the SBS process and limited by SRS. Importantly, the regular AQS and irregular SQS pulses are shown to differ tremendously: the former are much less intense (by more than an order of magnitude) than the latter. Pulses of these two kinds strongly interfere via competition to consume inversion in the system of Yb^{3+} ions, which is inherently a nonlinear process. A result of this is strong amplitude and timing (pulse separating in a pulses' train) jitter. Note that it was also found [36] that, even at higher AOM repetition rates (tens to hundreds kHz), powerful and short SBS-SQS pulses can suddenly appear among the regular, low-amplitude, and longer AQS ones, which can be harmful for applications. Apparently, this aspect of pulsed operation of an YDFL with intra-cavity AOM operating at low repetition rates, recognized for the first time to the best of our knowledge and seemingly being a general property of such lasers, deserves attention and precautions.

An analysis of the pure SQS regime in the GTW-YDFL, resulting as well from interplay of the SBS/SRS processes, as was clearly proved, was performed as a natural following step in the study. We emphasize the main conclusion of this part, namely the determining role of intra-cavity losses in establishing high-quality SQS pulsing. At the experimental conditions we dealt with (certain values of the Yb-doped GTWave structure length, FBG coupler reflectivity and pump level), the range of losses permitting optimal operation of the laser at SBS-SQS was determined to be 35... 55 dB. At this range, a train of powerful (peak power of about 2 kW), reproducible in shape, short (~75 ns) pulses, with minimal amplitude and timing jitter values (not exceeding 5% and 7%, respectively) and a well-defined repetition rate, is released from the laser. Otherwise, i.e. outside this loss range, the parameters of pulsing degraded. As was revealed, the other essential phenomena—together with the SBS and SRS processes—involved in producing optimal laser oscillation are ASE and the strength or weakness of optical feedback.

The detailed exploration of the SQS operation of the GTW-YDFL and the resulting addition to the current understanding of the physics behind its appearance leads one to predict further measures towards the improvement of such a type of laser.

Acknowledgments

The authors appreciate partial financial support by '*Omics Research Ltd*' (Hong Kong, China); they are also grateful to Dr E M Paderin (Moscow/Hong Kong) for invaluable assistance and Dr N N Il'ichev (Moscow) for fruitful discussions. This work was supported in part by the Ministerio de Economía y Competitividad (Project TEC2008-05490) and by the Generalitat Valenciana (Project PROMETEO/2009/077).

References

[1] Okamoto Y, Kitada R, Uno Y and Doi H 2008 *J. Adv. Mech. Des. Syst. Manuf.* **2** 651
[2] Dudley J M, Genty G and Coen S 2006 *Rev. Mod. Phys.* **78** 1135
[3] Roy A, Laroche M, Roy P, Leproux P and Auguste J-L 2007 *Opt. Lett.* **32** 3299
[4] Cascante-Vindas J, Diez A, Cruz J L and Andres M V 2009 *Opt. Lett.* **34** 3628
[5] Shi W, Leigh M, Zong J and Jiang S 2007 *Opt. Lett.* **32** 949
[6] Shi W, Leigh M A, Zong J, Yao Z, Nguyen D T, Chavez-Pirson A and Peyghambarian N 2009 *IEEE J. Sel. Top. Quantum Electron.* **15** 377
[7] Huang J Y, Zhuang W Z, Huang W C, Su K W, Huang K F and Chen Y F 2011 *Opt. Express* **19** 9364
[8] Hakulinen T, Koskinen R and Okhotnikov O G 2008 *Opt. Express* **16** 8720
[9] Khurgin J B, Jin F, Solyar G, Wang C C and Trivedi S 2002 *Appl. Opt.* **41** 1095
[10] Cole B, Goldberg L, Trussell C W, Hays A, Schilling B W and McIntosh C 2009 *Opt. Express* **17** 1766
[11] Pan Z, Meng L, Ye Q, Cai H, Fang Z and Qu R 2009 *Opt. Express* **17** 3124
[12] Upadhaya B N, Chakravarty U, Kuruvilla A, Thyagarajan K, Shenoy M R and Oak S M 2007 *Opt. Express* **15** 11576
[13] Wang Y, Martinez-Rios A and Po H 2004 *Opt. Fiber Technol.* **10** 201
[14] Wang Y and Xu C-Q 2004 *IEEE J. Quantum Electron.* **40** 1583
[15] Chernikov S V, Zhu Y, Taylor J R and Gapontsev V P 1997 *Opt. Lett.* **22** 297
[16] Kerttula J, Filippov V, Chamorovskii Y, Golant K and Okhotnikov O G 2010 *Opt. Express* **18** 18543
[17] Salhi M, Hideur A, Chartier T, Brunel M, Martel G, Ozkul C and Sanchez F 2002 *Opt. Lett.* **27** 1294
[18] Grudinin A B, Payne D N, Turner P W, Nilsson L J A, Zervas M N, Ibsen M and Durkin M K 2004 *USA Patent* N6826335
[19] Melkumov M A, Bufetov I A, Kravtsov K S, Shubin A V and Dianov E M 2004 *Quantum Electron.* **34** 843
[20] Grukh D A, Levchenko A E, Kurkov A S and Paramonov V M 2005 *Quantum Electron.* **35** 442
[21] Chen L R and Gu X 2007 *Opt. Express* **15** 5083
[22] Kurkov A S 2007 *Laser Phys. Lett.* **4** 93
[23] Kobtsev S M, Kukarin S V and Fedotov Y S 2008 *Laser Phys.* **18** 1230
[24] Kobtsev S M, Kukarin S V and Fedotov Y S 2008 *Opt. Express* **16** 21936
[25] Kir'yanov A V, Klimentov S M, Mel'nikov I V and Shestakov A V 2009 *Opt. Commun.* **282** 4759
[26] Kir'yanov A V and Il'ichev N N 2011 *Laser Phys. Lett.* **8** 305
[27] Hideur A, Chartier T, Ozkul C and Sanchez F 2000 *Opt. Commun.* **186** 311

[28] Renaud C C, Offerhaus H L, Alvarez-Chavez J A, Nilsson J, Clarkson W A, Turner P W, Richardson D J and Grudinin A B 2001 *IEEE J. Quantum Electron.* **37** 199
[29] Wang Y and Xu C-Q 2007 *Prog. Quantum Electron.* **31** 131
[30] Richardson D J, Nilsson J and Clarkson W A 2010 *J. Opt. Soc. Am.* B **27** B63
[31] Leng J Y, Wang X L, Xiao H, Zhou P, Ma Y X, Guo S F and Xu X J 2012 *Laser Phys. Lett.* **9** 532
[32] Kovalev V and Harrison R G 2002 *Opt. Commun.* **204** 349
[33] Spirin V V, Lopez-Mercado C A, Megret P and Fotiadi A A 2012 *Laser Phys. Lett.* **9** 377
[34] Dammig M, Zinner G, Mitschke F and Welling H 1993 *Phys. Rev.* A **48** 3301
[35] Ilichyov N N, Malyutin A A and Pashinin P P 1982 *Quantum Electron.* **9** 1803
[36] Barmenkov Yu O, Kir'yanov A V and Andres M V 2012 *IEEE J. Quantum Electron.* **48** 1484